Available online at www.sciencedirect.com

SCIENCE DIRECT®

ELSEVIER

International Journal of Heat and Mass Transfer 48 (2005) 2242–2249

International Journal of HEAT and MASS TRANSFER

www.elsevier.com/locate/ijhmt

CHF characteristics of R-134a flowing upward in uniformly heated vertical tube

Chang Ho Kim *, Soon Heung Chang

Korea Advanced Institute of Science and Technology, 373-1, Guseong-dong, Yuseong-gu, Daejeon 305-701, Republic of Korea

Received 27 August 2004; received in revised form 30 December 2004
Available online 26 February 2005

Abstract

An experimental study of the critical heat flux (CHF) using R-134a in uniformly heated vertical tube was performed and 182 CHF data points were obtained from the present work to investigate the CHF characteristics of R-134a. The investigated flow parameters in R-134a were: (1) outlet pressures of 13, 16.5, 23.9 bar, (2) mass fluxes of 285–1300 kg/m^2 s, (3) subcooling temperatures of 5–40 °C. The CHF tests were performed in a 17.04 mm I.D. test section with heated length of 3 m. The parametric trends of CHF show a general agreement with previous understanding in the water. To assess the suitability of the CHF test using R-134a for modeling the CHF in water, Bowring correlation and Katto correlation were used in the present investigation. It was found that the present test results coincided well with the data predicted with both correlations. It demonstrates that the R-134a can be used as the CHF modeling fluid of water for the investigated flow conditions and geometric condition.

Keywords: R-134a; CHF; CHF correlation; Fluid-to-fluid model; Forced convective boiling

1. Introduction

The critical heat flux (CHF) is the heat flux at which boiling crisis occurs and a sudden deterioration of heat transfer rate occurs. Therefore, critical heat flux of forced convective boiling is a phenomenon that has been thought as one of the most important parameters in designing and operating the heat transfer equipments with a high heat flux such as once-through boiler, evaporator, superconducting magnets, electronic equipment, rocket engines and so on. Great quantities of experimental and theoretical studies concerning CHF in water under forced convective boiling conditions have been performed over last 50 years. As a result of these efforts, a lot of methodologies have been developed to predict the CHF and its characteristics with some uncertainty [1–6]. There are several empirical prediction methods useful for different types of fluid [5,6]. Although many aspects of CHF have been understood to some extent, experimental investigations are usually limited to the simplified geometry due to the high expenditure and complexity. Particularly, to develop with the minimum cost the new fuel design in nuclear power plants, smaller scaled CHF tests on electrically heated rods are usually performed. Recently, many different techniques have been considered for increasing CHF in forced convection to increase the efficiency and safety margin of heat

* Corresponding author. Tel.: +82 42 869 3856; fax: +82 42 869 3810.
E-mail addresses: hokim4@kopec.co.kr, musoyou@kaist.ac.kr (C.H. Kim), shchang@kaist.ac.kr (S.H. Chang).

0017-9310/$ - see front matter © 2005 Elsevier Ltd. All rights reserved.
doi:10.1016/j.ijheatmasstransfer.2004.12.025

Nomenclature

D	inside diameter (m)
F_G	mass flux scaling ratio
$F_{\Delta h}$	latent scaling ratio
F_Q	heat flux scaling ratio
G	mass flux (kg/m^2 s)
G_P	mass flux of prototype fluid (kg/m^2 s)
G_M	mass flux of modeling fluid (kg/m^2 s)
h_{fg}	latent heat (kJ/kg)
Δh	inlet subcooling enthalpy (kJ/kg)
L	heated length (m)
LHS	left hand side
Min.	minimum
P	pressure (bar)
q_c	critical heat flux (kW/m^2)
q_{co}	q_c for $\Delta h = 0$ (kW/m^2)
RHS	right hand side
RMS	root mean square

Greek symbols

ρ	density of fluid (kg/m^3)
μ	dynamic viscosity of fluid (Pa s)
σ	surface tension (N/m)

Subscripts

f	saturated liquid
g	saturated vapor
M	modeling fluid
P	prototype fluid

transfer devices. But, due to the high latent heat and high critical pressure of water, CHF experiments in water are very expensive and confined in scale. Therefore, CHF in fluid with low latent heat and low critical pressure has been investigated, and several fluid modeling technologies have been developed [7–11]. Specially, in the development of new nuclear fuel design, CHF using the Freon instead of water has been researched at the stage of its feasibility study. The CHF studies by using the modeling fluids such as Freon have been investigated with two types of approaches. One is the dimensional analysis approach made by Barnett and Wood [10], Ahmad [7], and the other empirical approach initiated by Stevens et al. [9]. Katto has extensively studied CHF for forced convective boiling with different working fluids and presented the generalized correlations of CHF of flow boiling in uniformly heated vertical tubes [5,13]. At the same time, Shah also presented a graphical correlation to predict CHF covering 11 fluids for a wide range of flow conditions from subcooled to high quality [14] and later developed the generalized correlation covering a very wide range and yielding satisfactory prediction with the overall mean uncertainty of about 16% [6].

In CHF investigation using modeling fluid, the refrigerant, R-12 had extensively been used to model the CHF characteristics of water due to its low latent heat, low critical pressure, and well known properties [15]. However, it has been known that CFC (clorofluorocarbon) family such as R-12, R-12, R-133, R-144, etc., could deplete the ozone layer. The refrigerants such as R-134a and R-152a have been evaluated as an alternative in modeling CHF in water due to its harmlessness on the environment [12,16]. Particularly, since the thermo-physical properties of R-134a are close to R-12, R-134a is considered to be a new modeling fluid. CHF experiments using R-134a have been conducted only by a few researchers [12,17]. Particularly, Tain and Cheng reported that the CHF test data in R-134a agreed very well with the CHF data predicted by converting the standard CHF look-up table from water to R-134a equivalent condition [12]. These CHF experiments using R-134a cover a narrow flow condition and particular tubes with relatively small diameters and short heated length. Since the tubes used in once-through boiler have the long heated length and the inside diameter above 10 mm, the further investigations are needed to ensure that R-134a has the suitability as a CHF modeling fluid of water for the unexplored geometric conditions.

The main objective of this study is to provide an R-134a CHF database and to investigate the CHF characteristics of the R-134a in vertical tube covering a wide range of flow conditions and having the long heated length and large diameter. This schematic CHF test using R-134a is used to examine the suitability of R-134a as a CHF modeling fluid of water in the long heated tubes with a relatively large diameter. Also, this CHF data basis will be used as a reference for future rib effect studies on CHF and to provide physical insight for CHF enhancement mechanism in the rifled tube, which is key to the design of once-through boiler. The experimental data obtained from this study were compared with two different CHF prediction methods to assess the suitability of the CHF test data using R-134a for prediction of the CHF in water.

2. Experimental apparatus and procedure

2.1. Experimental loop

The CHF experiments were performed in Korea Advanced Institute of Science and Technology (KAIST) Freon test facility. The apparatus of the present

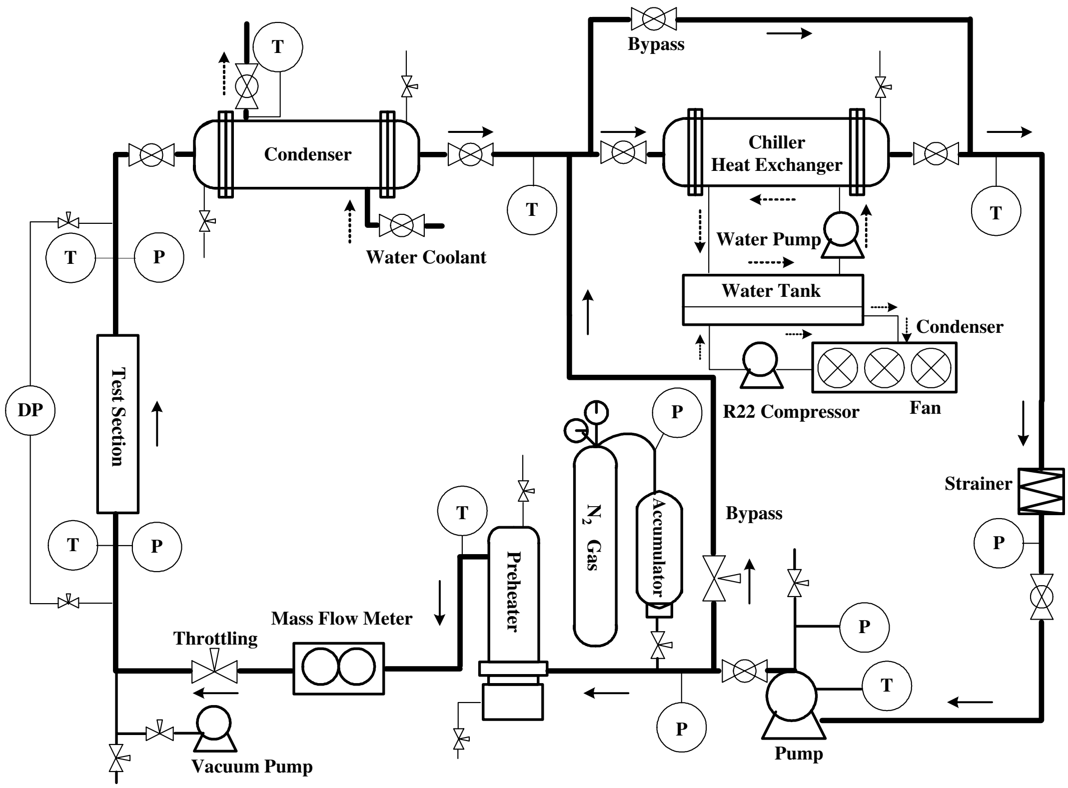

Fig. 1. Schematic diagram of the experimental system [5]. P: pressure instrumentation; T: temperature instrumentation and DP: differential pressure instrumentation.

experiment is schematically shown in Fig. 1 [18]. The R-134a experimental loop consists of the following components: a test section for CHF, a mass flow meter, a preheater for inlet subcooling control, an accumulator for pressure control, a canned pump for stable mass supply, a condenser, and a chilling system with R-22 and water–propylene glycol. An adjusting valve is used to precisely control flow rate to the test section. The loop is filled with R-134a in the vacuum condition. The test loop is designed for pressure of 30 bar and 200 °C. The loop flow is measured by the mass flow meter calibrated to be 2% of RMS error by manufacturer. Temperatures and pressures are measured at various locations as indicated by *T* and *P*, respectively, in Fig. 1.

2.2. Test section

The test section is schematically shown in Fig. 2 and is carbon steel (SA182) tube with upward flow. The tube is electrically heated directly with a DC power supply, which controls the power by a power transformer with silicon controlled rectifiers (SCRs) with the maximum power capacity of 40 V and 5000 A. The heated length of test section is 3000 mm and the inside and outside

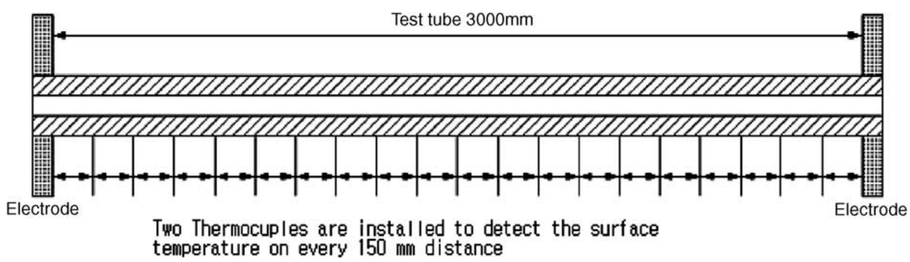

Fig. 2. Schematic diagram of test section.

diameters are 17.04 mm and 22.59 mm, respectively. These geometric dimensions are selected to reflect the actual tube used in a commercial boiler. The temperatures of the liquid at the inlet and outlet of the test section are measured with the in-stream T-type sheathed thermocouples. The temperatures of the outside wall are measured at 20 locations along the channel wall, and two K-type thermocouples are installed at each location. The first two thermocouples are located 5 mm below from the end of upper power clamp. Outlet pressure and inlet pressure are measured with pressure transducers and calibrated to be 0.5% of RMS error for a full range.

A pair of clamp-type copper electrodes grabs both ends of the test tube. Test section is connected to the flange, which is insulated from other part of the test loop with Teflon. The supplied current and the voltage difference between both ends of the test section are measured and collected by a data acquisition system.

2.3. Test procedure and test matrix

The flow direction is vertically upward. For all test conditions, the CHF data were taken. All process data including the tube wall temperatures were collected by a data acquisition system for later analysis. Before each series of experiments, a heat balance test was performed and showed that the heat losses were within 2.5%. First, the pump starts and the mass flow is controlled by the speed control with the converter and the control valve at a certain level. The test pressure in the test loop is increased by turning on the pre-heater and continuously increasing its power. After the pressure in the test loop reaches a pre-determined level, the inlet temperature is controlled by the power control to the pre-heater. The power to test section is increased at first rapidly to about 85% of CHF and then slowly. When the power is supplied to test section, the system pressure is controlled by venting the nitrogen gas in two accumulators. Boiling crisis is considered to occur when the wall temperature just below the upper power terminal is suddenly increased.

Table 1 summarizes the test matrix and the equivalent water-based conditions. The test conditions are selected by considering the startup condition of once-through boiler of a fossil power plant and the capacity of KAIST test loop. The inlet subcooling temperatures are 5–40 °C. Those test parameters would result in the dryout-type CHF which occurs in the rifled tube of once-through boiler.

3. Fluid-to-fluid scaling

Ahmad introduced the seven dimensionless parameters to represent the CHF based on dimensional analysis as follows [7]:

$$\frac{q_c}{Gh_{fg}} = f\left(\frac{L}{D}, \frac{\rho_f}{\rho_g}, \frac{\Delta h}{h_{fg}}, \frac{\mu_f}{\mu_g}, \frac{\mu_f^2}{\sigma D \rho_f}, \frac{GD}{\mu_f}\right) \tag{1}$$

The dimensionless parameter in LHS of Eq. (1) is a boiling number to represent the CHF and shall be equal with each the scaling fluid. In the general CHF test, the following three similarities can easily be obtained.

- Geometric similarity:

$$\left[\frac{L}{D}\right]_P = \left[\frac{L}{D}\right]_M \tag{2}$$

- Hydrodynamic similarity:

$$\left[\frac{\rho_f}{\rho_g}\right]_P = \left[\frac{\rho_f}{\rho_g}\right]_M \tag{3}$$

- Thermodynamic similarity:

$$\left[\frac{\Delta h}{h_{fg}}\right]_P = \left[\frac{\Delta h}{h_{fg}}\right]_M \tag{4}$$

where P means the prototype fluid and M means the modeling fluid.

Since it is almost impossible to make the individual parameter for the others be equal among scaling fluids, three parameters in RHS of Eq. (1) are combined into one scaling parameter. The scaling parameter has been expressed in various ways, depending on the investigators such as Ahmad [7], Dix [8], Katto [13], and Stevens and Kirby [21]. Since Katto's scaling parameter has been

Table 1
Test matrix condition in R-134a and their water-equivalent conditions

Pressure (bar)		Saturated temperature (°C)		Mass flux (R-134a) (kg/m^2 s)				
				285	500	712	1000	1300
R-134a	Water	R-134a	Water	Mass flux (water) (kg/m^2 s)				
13	70	49.4	295	402.1	705.4	1004.5	1410.8	1834.0
16.5	100	59.2	311	400.4	702.4	1000.2	1404.8	1826.3
23.9	140	75.5	336.6	396	695.3	990.1	1390.6	1807.7

successfully used for a scaling law, the present study uses the Katto's additional hydrodynamic similarity and is expressed as follows:

$$\left[\frac{G\sqrt{D}}{\sqrt{\sigma\rho_f}}\right]_P = \left[\frac{G\sqrt{D}}{\sqrt{\sigma\rho_f}}\right]_M \tag{5}$$

The following procedures can be used to convert the thermal–physical CHF properties from the modeling fluid to the prototype fluid.

(1) Calculate the density ratio of the liquid to the vapor. Find out the pressure at which the density ratio of prototype is equal to that of model fluid.
(2) Calculate the mass ratio at the equivalent pressure as follows:

$$F_G = \frac{G_P}{G_M} = \frac{\left(\sqrt{\sigma\rho/D}\right)_P}{\left(\sqrt{\sigma\rho/D}\right)_M} \tag{6}$$

(3) Calculate the latent scaling ratio defined as latent ratio of prototype fluid to vapor of model fluid as follows:

$$F_{\Delta h} = \frac{(h_{fg})_P}{(h_{fg})_M} \tag{7}$$

(4) Calculate the heat flux scaling ratio by multiplying the latent scaling ratio and the heat flux scaling ratio as follows:

$$F_Q = F_G \times F_{\Delta h} \tag{8}$$

(5) Calculate the critical heat flux from the heat flux scaling ratio as follows:

$$(q_c)_P = F_Q \times (q_c)_M \tag{9}$$

4. CHF test results and discussion

Figs. 3 and 4 show the effect of the inlet subcooling enthalpy on CHF at different flow conditions. The results are obtained at the pressure of 13, 16.5 and 23.9 bar and at the mass flux of 285, 500, 712, 1000 and 1300 kg/m^2 s. The CHF increases almost linearly with the inlet subcooling enthalpy, but the effect decreases with decreasing mass flux. Fig. 5 shows the effect of the pressure on CHF, indicating that CHF decreases with increasing the pressure. These trends agree with the general understanding in the water [19].

Fig. 6 shows the CHF vs. the critical quality graph for the two flows ($G = 500$ and 1000 kg/m^2 s) and pressures of 13, 16.5 and 23.9 bar. This figure shows that:

- A CHF value decreases continuously with an increase of the critical quality without a sharp change in slope on the CHF vs. critical quality.

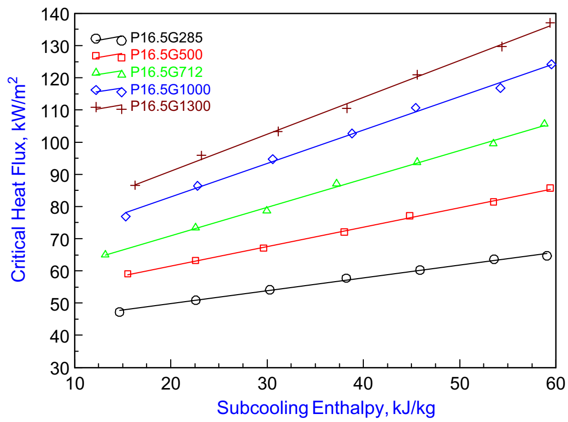

Fig. 3. Effect of inlet subcooling enthalpy on CHF of R-134a in vertical tube (outlet pressure: 16.5 bar).

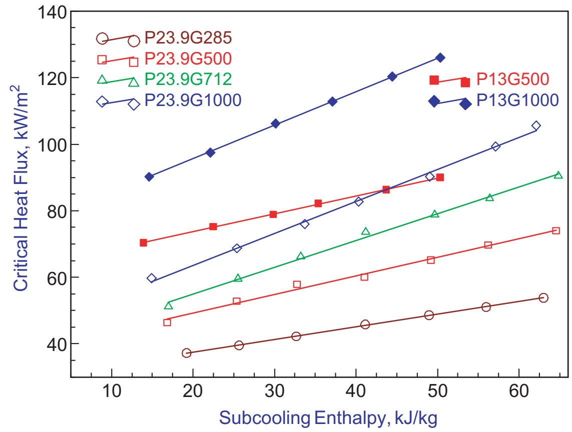

Fig. 4. Effect of inlet subcooling enthalpy on CHF of R-134a in vertical tube (outlet pressures: 13 bar and 23.9 bar).

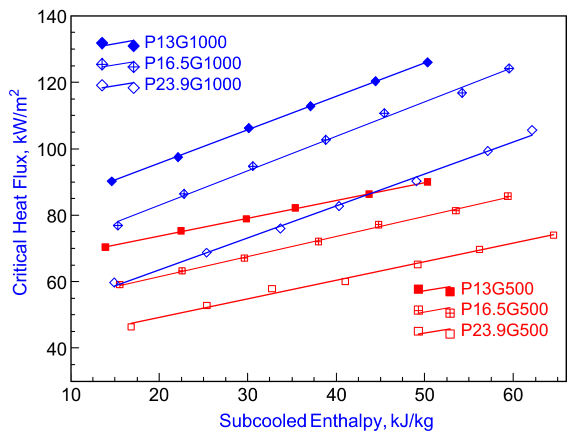

Fig. 5. Effect of system pressure on CHF of R-134a in vertical tube ($G = 500$ and 1000 kg/m^2 s).

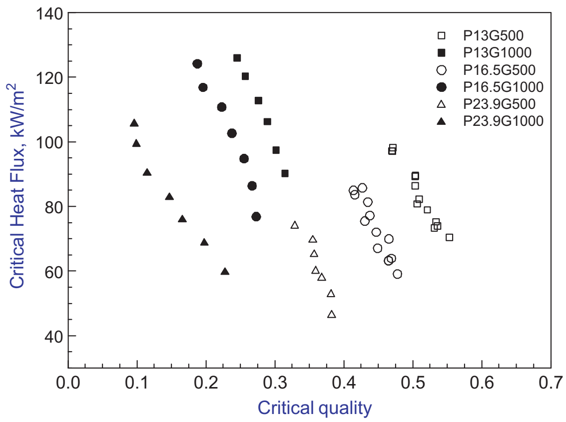

Fig. 6. Effect of critical quality on CHF of R-134a in vertical tube ($G = 500$ and $1000\ \mathrm{kg/m^2\,s}$).

- Although the test data cover the narrow range of critical qualities, the CHF values at the higher mass flux ($G = 1000\ \mathrm{kg/m^2\,s}$) is considered to be lower than those at the lower mass flux ($G = 500\ \mathrm{kg/m^2\,s}$) in consideration of the data trends at each test condition. It indicates that the inverse mass flux effects [22] are present for all test pressures.

For comparing with the present experimental data, two different prediction methods are used: (1) correlation of Bowring and (2) generalized correlation of Katto because these correlations are known as good prediction methods covering a wide range of flow conditions and tube geometry. Since one correlation is applicable only for the water, and the other is generally applicable, its approach is considered to be adequate to assess the suitability of R-134a as a CHF modeling fluid of water.

4.1. Bowring's prediction method

The correlation of Bowing was developed for CHF in water and based on the inlet condition [2]. The basic equation for CHF is:

$$q_c = \frac{A' + 0.25DG\,\Delta h_i}{C' + L} \qquad (10)$$

where

$$A' = \frac{0.5792 h_{fg} DGF_1}{1 + 0.0143 F_2 D^{0.5} G}, \quad C' = \frac{0.077 F_3 DG}{1 + 0.347 F_4 (G/1356)^n}$$

F_1, F_2, F_3, F_4 and n are function of a non-dimensional pressure, $P' = P/68.95$.

$$n = 2 - 0.5P' \qquad (11)$$

Since the water-equivalent pressures tested in this study are greater than 68.95 bar,

$$F_1 = P'^{-0.368} \exp[0.648(1 - P')] \qquad (12)$$

$$F_1/F_2 = P'^{-0.448} \exp[0.245(1 - P')] \qquad (13)$$

$$F_3 = P'^{0.219} \qquad (14)$$

$$F_4 = F_3 P'^{1.649} \qquad (15)$$

The correlation of Bowring is applicable for the pressure of 2–190 bar, tube diameter of 2–45 mm, tube length 0.15–3.7 m and mass flux of 136–18 600 $\mathrm{kg/m^2\,s}$. 3800 data points were used to develop the correlation, and the RMS error of the prediction are 7%. Since this correlation is applicable for only water, the present CHF data of R-134a are first converted into water-equivalent values using thermal–physical properties of the water and R-134a. 182 data points are used for comparison with the prediction method. Fig. 7 shows the comparison of the water-equivalent CHF data converted from the CHF data in R-134a with the CHF prediction using Bowring correlation. The RMS error and average error of the prediction are 10.4% and −5.2%, respectively. A good agreement is achieved between the converted CHF and the predicted CHF. A systematical analysis reveals that the calculated CHF generally underestimates the CHF test results and the deviation depends on the system pressure. For 13, 16.5 and 23.9 bar, the average errors of the prediction CHF are 5.2%, −4.1% and −12.9%, respectively. It agrees with the CHF investigation in R-134a of Tain and Cheng, presented that for the high pressure the CHF prediction using fluid-to-fluid modeling resulted in under-prediction of CHF [12]. The reason for this is unknown, but it may be related to the possibility of the thermal decomposition of R-134a due to an increase of the heating surface temperature with increasing the system pressure.

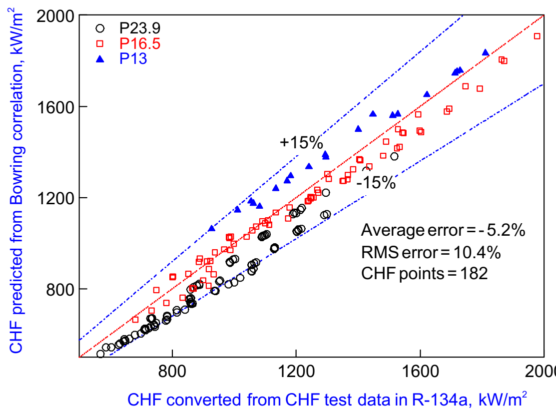

Fig. 7. Comparison of test results in vertical tube with Bowring correlation.

4.2. Katto's prediction method

Katto and Ohno presented the improved version of generalized CHF correlation of forced convective boiling in uniformly heated tubes covering various fluids based on the inlet condition [5]. The basic equation for CHF is:

$$q_c = q_{co}\left(1 + K\frac{\Delta h_i}{h_{fg}}\right) \tag{16}$$

Since the density ratio of vapor to liquid is less than 0.15 for the testing pressure range of this study, q_{co} is obtained from the minimum value as follows:

$$\frac{q_{co}}{Gh_{fg}} = \text{Min.}\left[\frac{CW^{0.043}}{L/D}, \frac{0.1(\rho_g/\rho_f)^{0.133}W^{1/3}}{1+0.0031(L/D)}, \frac{0.098(\rho_g/\rho_f)^{0.133}W^{0.433}(L/D)^{0.27}}{1+0.0031(L/D)}\right] \tag{17}$$

The non-dimensional parameter, K is obtained from the minimum values as follows:

$$K = \text{Min.}\left[\frac{0.261}{C(\sigma\rho_f/G^2L)^{0.043}}, \frac{(5/6)(0.0124+D/L)}{(\rho_g/\rho_f)^{0.133}W^{1/3}}\right] \tag{18}$$

where $W = \sigma\rho_f/G^2L$ and $C = 0.34$.

The correlation of Katto is applicable for the density ratio of 0.0003–0.41, tube diameter of 1–80 mm, tube length 0.01–8.8 m and W of 3.0×10^{-9}–2.0×10^{-2}. The RMS error of the prediction is 20%.

Fig. 8 shows the comparison of CHF test data in R-134a with the CHF data obtained by using the generalized correlation of Katto. The RMS error and average error of the prediction are 4% and +0.3, respectively. A very good agreement is achieved between the CHF test data and the predicted CHF data. A systematical analysis reveals that there is no dependency on the system pressure. Katto presented that there were four characteristic regimes of CHF, called L-, H-, N-, and HP-regime [13]. The CHF mechanism in the L-regime and H-regime mainly corresponds to the dryout-type under annular flow condition, the CHF mechanism in the N-regime mainly corresponds to the departure from nucleate boiling (DNB) concerned with a frothy or bubbly flow pattern, and HP-regime is a special regime when the system pressure is extremely high [20,22]. Fig. 9 shows that all experimental data investigated in this study belongs to H-regime except for the CHF data obtained at the pressure 23.9 bar with the mass flux 1300 kg/m^2 s. These data correspond to N-regime. Also, the critical quality range is from 0.02 to 0.72, and only the CHF data in N-regime have the critical qualities below 0.1. Based on these characteristic regimes of CHF and critical quality condition, it is ascertained that most of CHF data belongs to the dryout-type CHF except that a few of CHF data investigated at 23.9 bar belongs to DNB type.

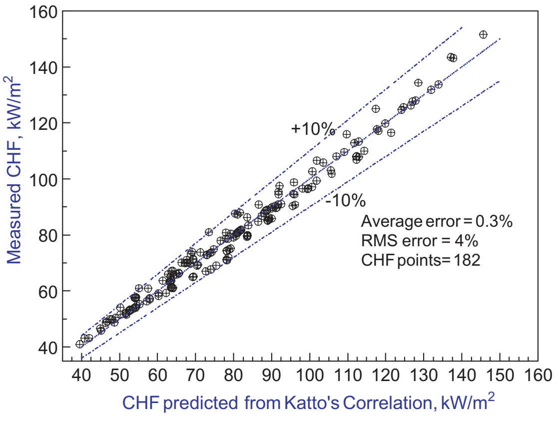

Fig. 8. Comparison of test results in vertical tube with Katto's correlation.

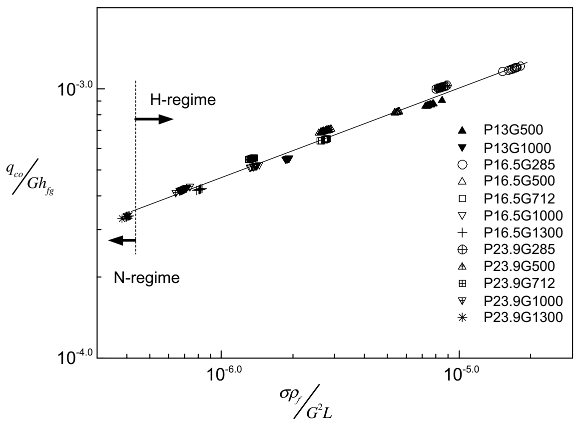

Fig. 9. CHF characteristics of R-134a (H-regime and N-regime).

5. Conclusions

Experiment for critical heat flux using R-134a in vertical uniformly round tubes was performed and 182 CHF data points were obtained from the present work. The investigated flow parameters in R-134a was: (1) outlet pressures of 13, 16.5, 23.9 bar, (2) mass fluxes of 285–1300 kg/m^2 s, (3) inlet subcooling temperatures of 5–40 °C. The CHF tests were performed in a 17.04 mm I.D. test section with heated length of 3 m. The critical quality range is from 0.02 to 0.72.

(1) The parametric trends of CHF in R-134a show a general agreement with previous understanding in the water. Also, the inverse mass flux effects are present under all test pressure conditions.

(2) To assess the suitability of the R-134a as a CHF modeling fluid of water in the 3 m length tube with a inside diameter of 17.04 mm, Bowring correlation and Katto correlation are used in the present investigation. Both correlations results in a good agreement with the water-equivalent present CHF data. This schematic CHF test with R-134a shows that R-134a can be used as a CHF modeling fluid of water in the long heated tubes with a relatively large diameter.
(3) The Bowing's prediction generally underestimates the CHF values and the deviation depends on the system pressure. The further researcher work to investigate the reason is necessary.
(4) A very good agreement is achieved with Katto correlation regardless of the flow conditions. Based on the characteristic regimes of CHF and critical quality condition, it is ascertained that most of CHF data belongs to the dryout-type CHF except that a few of CHF data investigated at 23.9 bar belongs to DNB type.

Acknowledgments

This work was sponsored by Doosan Heavy Industries and Construction Co., Ltd. and the "*National Laboratory*" program of the Korean Ministry Of Science and Technology (MOST). The authors would like to express their appreciation to Dr. Y.H. Jeong and Dr. I.C. Bang of KAIST and to Dr. S.Y. Chun and Dr. S.K. Moon of KAERI.

References

[1] L.S. Tong, H.B. Currin, A.G. Thorpe II, New correlations predicted DNB conditions, Nucleonics 21 (5) (1963) 43.
[2] R.W. Bowring, A simple but accurate round tube uniform heat flux, dry-out correlation over the pressure range, 0.7–12 MN/m^2 (100–2500 psia), AEEW-R789.
[3] K.M. Becker, D. Djursing, K. Lindberg, O. Eklind, C. Osterdahl, Burnout conditions for round tubes at elevated pressures, in: Proc. Int. Symp. on Two-Phase Systems, Haifa, Israel, 1972, pp. 55–73.
[4] D.C. Groeneveld, P.L. Kirillov et al., The 1995 look-up table for critical heat flux in tubes, Nucl. Eng. Des. 163 (1996) 1–23.
[5] Y. Katto, H. Ohno, An improved version of the generalized correlation of critical heat flux for the forced convective boiling in uniformly heated vertical tubes, Int. J. Heat Mass Transfer 27 (1984) 1641–1648.
[6] M.M. Shah, Improved general correlation for critical heat flux during upflow in uniformly heated vertical tubes, Int. J. Heat Fluid Flow 8 (1987) 325–335.
[7] S.Y. Ahmad, Fluid to fluid modeling of critical heat flux: a compensated distortion model, Int. J. Heat Mass Transfer 16 (1973) 641–662.
[8] G.E. Dix, Freon-water modeling of CHF in round tubes, ASME-Paper No. 70-HT-26, 1970.
[9] G.F. Stevens, D.F. Elliot, R.W. Wood, An experimental investigation into forced convection burn-out in Freon with reference to burn-out in water uniformly heated round tubes with vertical up-flow, AEEW-R 321, 1964.
[10] P.G. Barnett, R.W. Wood, An experimental investigation to determine the scaling laws of forced convection boiling heat transfer, Part 2, AEEW-R443, 1965.
[11] P.G. Barnet, An investigation into the validity of certain hypothesis implied by various burnout correlation, UKAEA Report AEEW-R 214, 1963.
[12] R.M. Tain, S.C. Cheng, Critical heat flux measurements in a round tube for CFCs and CFC alternatives, Int. J. Heat Mass Transfer 6 (8) (1993) 2039–2049.
[13] Y. Katto, A generalized correlation of critical heat flux for the forced convective boiling in vertical uniformly heated round tubes, Int. J. Heat Mass Transfer 21 (1978) 1527–1542.
[14] M.M. Shah, A generalized graphical method for predicting CHF in uniformly heated vertical tubes, Int. J. Heat Mass Transfer 22 (1979) 557–568.
[15] X. Cheng, F.J. Erbacher, U. Muller, Critical heat flux in uniformly heated vertical tubes, Int. J. Heat Mass Transfer 40 (1997) 2929–2939.
[16] J.R. Thome, Two-phase heat transfer to new refrigerants, in: Proc. 10th Int. Conf. Multiphase Flow, 1994, pp. 19–41.
[17] I.L. Pioro, D.C. Groeneveld et al., Comparison of CHF measurements in R-134a cooled tubes and the water CHF look-up table, Int. J. Heat Mass Transfer 44 (2001) 73–88.
[18] I.C. Bang, S.H. Chang, W.P. Baek, Visualization of the subcooled flow boiling of R-134a in a vertical rectangular channel with an electrically heated wall, Int. J. Heat Mass Transfer 47 (2004) 4349–4363.
[19] S.K. Moon, W.P. Baek, S.H. Chang, Parametric trends analysis of the critical heat flux based on artificial neural network, Nucl. Eng. Des. 163 (1996) 29–49.
[20] Y. Katto, On the heat flux/exit-quality type correlation of the CHF of forced convective boiling in uniformly heated round tubes, Int. J. Heat Mass Transfer 24 (1980) 533–539.
[21] G.F. Stevens, G.J. Kirby, A quantitative comparison between burn-out data for water at 1000 lb/in^2 and Freon-12 at 155 ln/in^2 (ABS) uniformly heated round tubes, vertical upflow, UKAEA Report, AEEW-R 327, 1964.
[22] Y. Katto, An analytical investigation on CHF of flow boiling in uniformly heated vertical tubes with special reference to governing dimensionless groups, Int. J. Heat Mass Transfer 25 (1982) 1353–1361.